Discrete Molecular Dynamics Study of Alzheimer Amyloid β-protein (Aβ) Folding

Alfonso R. Lam[*1], Brigita Urbanc[*], Jose M. Borreguero[$\diamond$], Noel D. Lazo[†], David B. Teplow[†], and H. Eugene Stanley[*]

[*] *Department of Physics, Center for Polymer Studies, Boston University, Boston, MA 02215*

[$\diamond$] *Center for the Study of System Biology, Department of Biology, Georgia Institute of Technology, Atlanta GA 30318*

[†] *Department of Neurology, David Geffen School of Medicine, and Molecular Biology Institute and Brain Research Institute, University of California, Los Angeles, CA 90095*

ABSTRACT

Aβ folding and assembly are believed to be seminal pathogenic events in Alzheimer's disease. We study Aβ(1-42) folding by discrete molecular dynamics using a four-bead protein model with hydrogen bonds and amino acid-specific interactions. Interactions account for hydrophobic/hydrophilic effect that mimic the solvent as well as electrostatic effects. We study monomer conformations on a wide temperature range. At each temperature, we find many different monomer conformations, indicating that Aβ(1-42) folding is not unique. At low temperatures, we observe globular conformations with some α-helical content while at higher temperatures β-strand-rich conformations with no α-helical content are present. This temperature-driven conformational change is consistent with experimental findings by Gursky and Aleshkov. Varying the strength of electrostatics interactions, we show that all monomer conformations become more compact. β-strand-rich conformations are characterized by turn regions centered at D23-K28 and G37-G38, and β-strands at L17-A21, I31-V36 and V39-A42, which are important in fibril formation.

Keywords: Alzheimer's disease, amyloid β-protein, protein folding, discrete molecular dynamics.

I. INTRODUCTION

   Alzheimer's disease (AD) is a progressive neurological disorder that is estimated to affect 50% of humans aged 85 and older. AD is characterized by extracellular senile plaques, intracellular neurofibrillary tangles, and substantial neuronal loss. Senile plaques are made of fibrillar aggregates of the amyloid β-protein (Aβ). Aβ is produced normally in the body predominately in two forms, Aβ(1-40) and Aβ(1-42), that differ structurally by the absence or presence of two C-terminal amino acids, respectively. One of the leading hypotheses of AD etiology is the "amyloid cascade hypothesis," which posits that self-assembly of Aβ is a seminal pathogenetic event [1, 2]. The initial stages of the assembly process produce small oligomers that may be the proximate neurotoxins in the disease (for reviews, see Refs. [3, 4]). Aβ(1-42) is particularly prone to aggregation [5], appears to be the more toxic of the two Aβ alloforms [6], and is linked to familial (genetic) forms of AD [7].

   The idea of applying the DMD approach to study protein folding and aggregation was proposed in 1996 [8]. Since then numerous studies have developed and applied the DMD approach to study protein folding [9–13]. Peng et al. studied the aggregation of 28 Aβ(1-40) monomers into a β-sheet aggregate using a two-bead amino acid model with Gō interactions [14]. Urbanc et al. studied Aβ(1-40) and Aβ(1-42) dimer formation using all-atom MD with implicit solvent/explicit solvent that incorporated a four-bead amino acid model and hydrogen bond interactions [15]. In a subsequent study, Urbanc et al. applied the DMD approach to study differences in oligomer formation between Aβ(1-40) and Aβ(1-42) [16]. Borreguero et al. applied a united-atom DMD model, in which all atoms except hydrogens are present, to study folding events of Aβ(21-30), a decapeptide segment of Aβ hypothesized to nucleate monomer folding [17].

   We present here results of our DMD study of Aβ(1-42) folding. We use a four-bead amino acid model with hydrogen bonding, amino acid-specific interactions that account for solvent implicitly, and electrostatic interactions. Our results show that a folded Aβ(1-42) monomer adopts a collapsed coil structure with a small amount of α-helix at low temperatures and a β-strand rich conformation at higher temperatures. We discuss our results in the framework of existing experimental and computational findings.

---

[1] Presenting author: e-mail: arlam@buphy.bu.edu

II. METHODS

A. Discrete Molecular Dynamics

Discrete molecular dynamics (DMD) is an efficient molecular dynamics method due to simplified interparticle potentials which are reduced to one or more square-wells [18]. A pair of particles moves with constant velocities along straight lines until a distance is reached at which the potential is discontinuous, and a collision occurs. At that moment, particle velocities and directions of motion are recalculated such that the total energy, momentum, and angular momentum are conserved. Because DMD is event-driven, it is faster than traditional molecular dynamics. To further increase the efficiency, DMD typically is used without explicit solvent and in combination with coarse-grained amino acid models.

B. Four-Bead Protein Model

We model Aβ using a four-bead model [19–21] that assigns to each amino acid up to four beads corresponding to amide N, α-carbon C_α, carbonyl C' groups, and up to one side-chain bead centered at the C_β group. There are three types of bonds in the model: *(i)* covalent bonds N—C_α, C_α—C', and C_α—C_β; *(ii)* peptide bonds C'—N that connect two neighboring amino acids in the sequence; and *(iii)* constraints that allow for a correct backbone geometry. Each bond is characterized by distance constraints $r_{min}^{AB} = D^{AB}(1-\sigma)$ and $r_{max}^{AB} = D^{AB}(1+\sigma)$, where D^{AB} is an average distance between beads A and B and σ is chosen to be 0.02. D^{AB} and the hardcore radii for the four beads were obtained phenomenologically using known protein structures from the PDB database [21].

C. Hydrogen Bonding and Amino Acid-Specific Interactions

In proteins, a backbone hydrogen bond (HB) is formed between a carbonyl oxygen (O) and an amide hydrogen (H) atom. In the four-bead model, the positions of O and H can be reconstructed knowing the positions of the three backbone groups N, C_α, and C'. A hydrogen bond is modeled between the amide N_i of the amino acid i and the carbonyl C_j' group of the amino acid j. N_i and C_j' can form a HB at a distance range [4 Å, 4.2 Å] if four additional constraints are satisfied. These constraints involve positions of C_{i-1}, N_i, and C_{α_i}, as well as C_{α_j}, C_j', and N_{j+1}, and account for the angular dependence of the HB (for a detailed description, see Ref. [21]). Once the bond is formed, the model implements a "hydrogen bond-type reaction" that changes N_i and C_j into N_i' and C_j' in the form $N_i + C_j \rightleftharpoons N_i' + C_j'$ to assure that the amino group N_i and the carbon group C_j cannot form any other hydrogen bond. In this study, we assign the potential energy of one HB, E_{HB}, a value of 1.0. E_{HB} represents a unit of energy in our model.

Because DMD is solvent-implicit, amino acid-specific interactions between the side chain beads are introduced in the four-bead model to mimic the solvent effects. Amino acids are characterized as hydrophobic, non-charged hydrophilic, or charged hydrophilic. We use a hydropathy scale by Kyte and Doolittle [22]. In our modeling, the hydrophobic amino acids are I, V, L, F, C, M, and A, non-charged hydrophilic amino acids are N, Q, and H, and charged hydrophilic amino acids are positively-charged R and K and negatively-charged E and D. Amino acids G, P, S, T, Y, and W are considered neutral. The effective hydrophobicity is introduced as an attractive interaction between two hydrophobic side chain beads, which minimizes their combined solvent accessible surface area (SASA). The effective hydrophilicity is introduced as a repulsive interaction between two non-charged hydrophilic beads or between a charged and a non-charged hydrophilic bead, which keeps these side chains apart and thus maximize their combined SASA. The neutral side chain beads interact with each other and with the rest of side chain beads only through hard core repulsion. These interactions are described by a single square-well potential between side chain beads C_β with a threshold distance of 7.5 Å. The strength of the hydropathic interactions is given by the potential energy between two isoleucines, E_{HP}, set here to 0.15. We model the electrostatic interactions between two charged side chain beads by a double attractive/repulsive square-well potential with a long interaction distance of 7.5 Å and a short interaction distance of 6.0 Å. We denote the electrostatic potential energy by E_{CH} and keep it below the potential energy of a HB, $E_{CH} < 1$.

D. Initial Conformations and Parameters Settings

We use three values of the electrostatic interaction (EI) strength E_{CH}, 0.0, 0.3, and 0.6. By running the DMD simulations of a single Aβ(1-42) peptide at a high temperature $T = 4.0$ we obtain the random coil-like conformations with average zero potential energies. These conformations are used as initial conformations in production runs. We acquire 100 different initial conformations for each of the three strengths of EI, E_{CH}. In the production runs, these conformations are subjected to a heat bath at a fixed temperature at a fixed volume in a cubic box of 200 Å.

E. Intramolecular Contact Map

In the analysis of our results, we calculate the average intramolecular contact maps at each temperature and at each strength of EI. When two beads are at a distance ≤ 7.5 Å, they are in contact. If C_{ij} is the number of contact pairs between amino acids i and j, then the average contact map at the position (i, j), $< C_{ij} >$, is defined as an average of all C_{ij} from different trajectories. Because a maximum number of beads per amino acid is 4, the maximum number of contacts between any two amino acid is 16. We normalize the contact maps to the same maximum value.

F. Secondary Structure Analysis

We use the STRIDE program [23] within the Visual Molecular Dynamics (VMD) software package [24] to determine the secondary structure propensity per amino acid of a given conformation. We then calculate the average over all conformations to determine the average propensity for a turn, β-strand, or an α-helix.

III. RESULTS

The primary structure of Aβ(1-42) is DAEFRHDSGYEVHHQKLVFFAEDVGSNKGAIIGLMVGGVVIA. We explore Aβ(1-42) monomer folding using a four-bead model with backbone hydrogen bonds and amino acid-specific interactions between the side chain beads. We study a wide temperature range $T \in [0.10, 0.18]$ at $E_{CH} = 0.0, 0.3$ and 0.6. At each temperature and for each EI strength we obtain 100 trajectories each starting from a different random coil-like, zero potential energy conformation. Our results show that at $0.10 < T < 0.12$, monomer conformations adopt a collapsed coil structure with loops and turns and some β-strand content. At each temperature and EI strength, we analyze the 100 final monomer conformations in terms of clustering with respect to the RMSDs and the TM-score function [25] (data not shown). Our results indicate that overall no particular families of conformations can be defined. Despite the lack of a well-defined folded structure, some average structural characteristics can be determined. Propensity for β-strand formation increases with temperature, and at $0.12 < T < 0.14$, monomer conformations adopt a more extended structure with a substantial β-strand content. By calculating a heat capacity in the temperature range $T \in [0.10, 0.18]$, we find that a transition into a random coil conformation occurs at $T \approx 0.145$ (for $E_{CH} = 0.0$ and 0.3) and at $T \approx 0.150$ (for $E_{CH} = 0.6$) (data not shown).
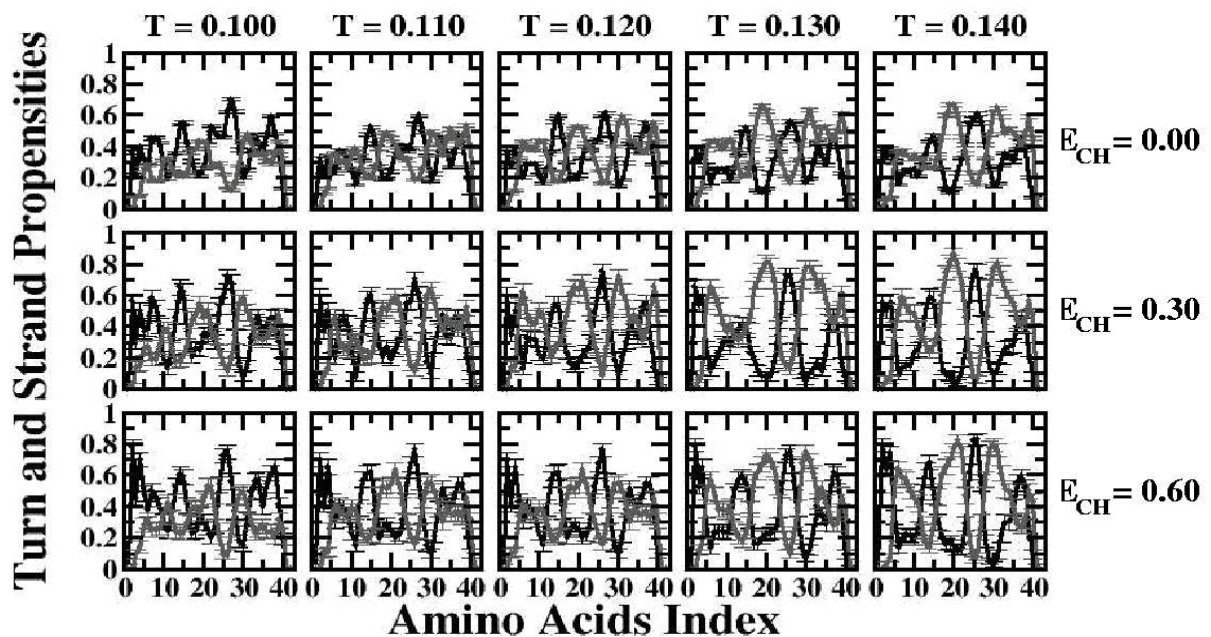
Secondary structure analysis is shown in Fig. 1. In Fig. 1a we show turn and β-strand propensities per amino acid at several selected temperatures and at three EI strengths. We observe an increase of the β-strand propensities with temperature in the central hydrophobic core (17-21), mid-hydrophobic cluster (30-36), and the C-terminal region (39-42). These β-strand propensities increase with the EI strength. We also find regions with pronounced turn propensities centered at 14-15, 25-26, and 36-38, and an additional turn region 2-4 that becomes pronounced only at the highest EI strength. The corresponding turn-like structures tend to be narrower in the presence of EI, consistent with a higher propensity for β-strand formation. The α-helix propensities are small overall and are zero at temperatures $T > 0.13$. At lower temperatures, where the conformation is a collapsed coil, the α-helix propensity is the highest, but does not exceed 8% in any protein region (Fig. 1b).

Intramolecular contact maps at several temperatures and three different EI strengths are shown in Fig. 2. These contact maps show pairs of amino acids that are close to each other. At low temperatures, we observe many contacts, in particular in hydrophobic parts of the protein—central hydrophobic core (17-21), mid-hydrophobic cluster (31-36), and the C-terminal cluster (39-42). There are two loop or turn regions, centered at G25-S26 and G37-G38. In the presence of EI, these two regions get more pronounced and narrower, and the number of contacts in the N-terminal region of the protein increases as well. As the temperature increases, the overall number of contacts is reduced due to increased thermal fluctuations. However, the two loop/turn regions remain. In the presence of EI, the loop/turn region centered at G25-S26 is narrower and characterized by more contacts because of the presence of strong EI between oppositely charged residues E22-K28 and D23-K28 that induces a local β-hairpin conformation.
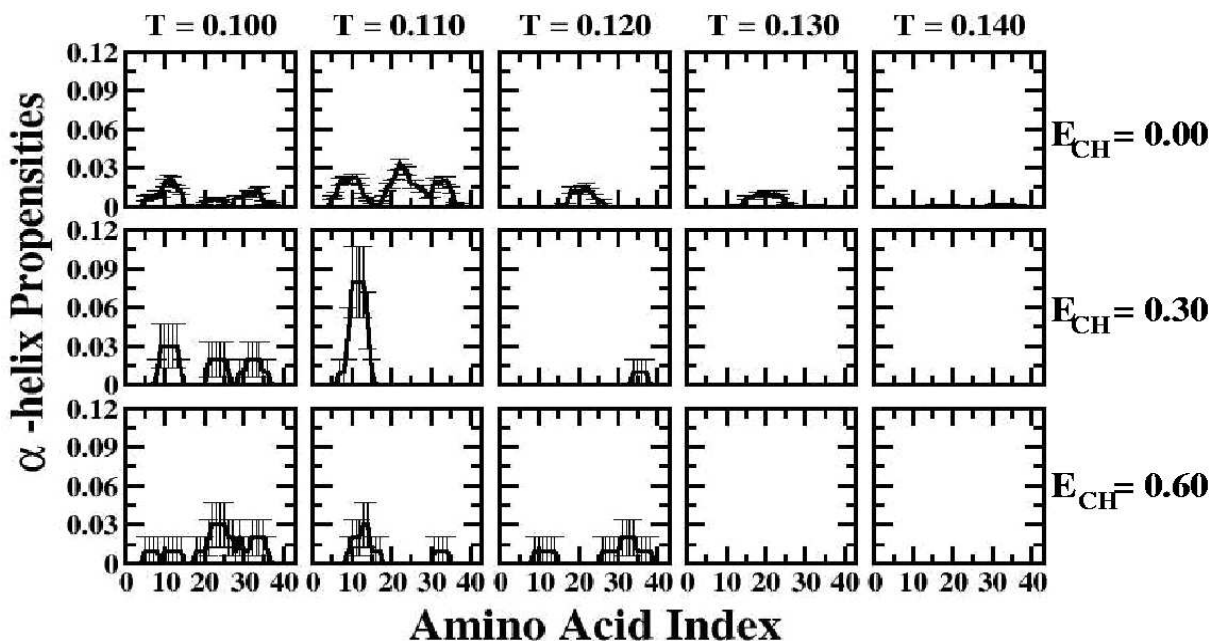
Selected typical conformations at different temperatures and different EI strengths are shown in Fig. 3. As determined by our analysis of the secondary structure and contact maps, we find a typical collapsed coil conformation at low temperatures (Fig. 3a). At a high temperature, we find substantial amounts of a β-sheet structure (Fig. 3b) that gets more pronounced when EI are present (Fig. 3c-d). We also calculated the average radius of gyration $\bar{R}_g$ as a function of temperature (data not shown). Our results show that $\bar{R}_g$ increases with temperature, consistent with a structural change from a collapsed coil to a more extended β-sheet structure. Interestingly, $\bar{R}_g$ decreases with the EI strength, indicating that the average monomer structure gets more compact.

IV. DISCUSSION

We analyze structural features of Aβ(1-42) monomer using DMD and a four-bead protein model with HB and amino acid-specific interactions which implicitly account for solvent water. Experimental studies of full-length Aβ monomers in water–organic solvent mixtures showed that the monomer structure consists of two α-helical regions connected through a flexible turn- or bend-like kink [26, 27]. NMR experiments on Aβ(10-35) monomer structure

FIG. 1: Average secondary structure propensities per amino acid of Aβ(1-42) monomer conformations at $T = 0.10, 0.11, 0.12, 0.13, 0.14$ and at $E_{CH} = 0.0$ (top row), $E_{CH} = 0.3$ (middle row), and $E_{CH} = 0.6$ (bottom row). (A) Turn (black) and β-strand (grey) propensities. (B) α-helix propensities.

in an aqueous solution show a collapsed structure with loops, strands, and turns without any significant amount of α-helical or β-strand content [28]. These studies suggest that Aβ monomer structure is very sensitive to external conditions, such as temperature, pH, and solvent. In our study, a collapsed structure with loops is observed at low temperatures, in agreement with a monomer structure in an aqueous solution observed by Zhang et al. [28]. We also show that this collapsed coil structure occurs coincident with some α-helical structure, however the α-helix propensity per amino acid does not exceed 8%.

At higher temperatures, the collapsed coil structure is converted into a β-sheet-like conformation with no α-helical
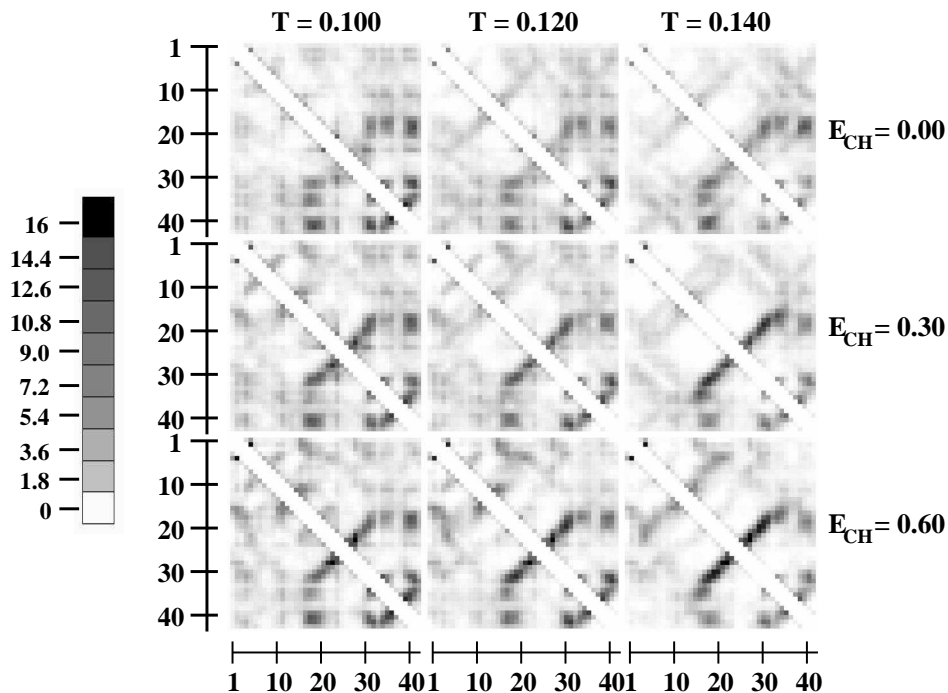
FIG. 2: Intramolecular contact maps for monomer at three different values of EI strength at three different temperatures. Both axes denote the amino acid indices. The colors correspond to the average number of contacts between two amino acids. The grey scale is presented on the left.
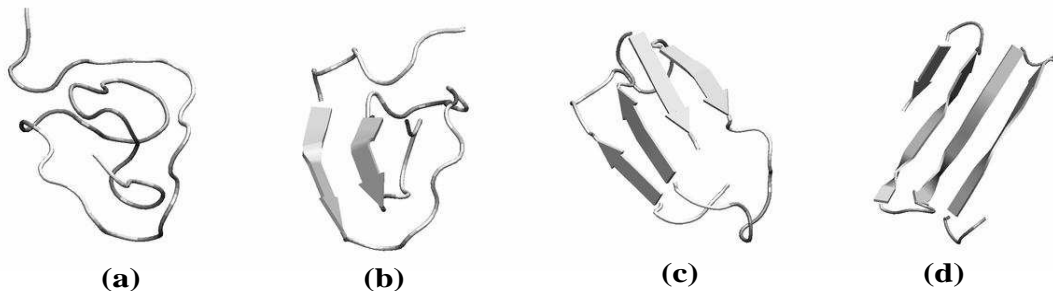

FIG. 3: Typical conformations at (a) $T = 0.10$ and (b-d) $T = 0.14$. The effect of EI is illustrated by comparing (b) $E_{CH} = 0.0$, (c) $E_{CH} = 0.3$, and (d) $E_{CH} = 0.6$. β-strands are presented by arrow ribbons. Figures were created using VMD software package [24].

content. The temperature-dependence of the Aβ(1-40) monomer and dimer structures in water was experimentally studied by Gursky and Aleshkov [29]. They observed an Aβ(1-40) monomer structure with little α-helix or β-strand at low temperatures. As the temperature was increased to physiological, substantial β-sheet content developed. This structural transition was not accompanied by oligomer formation, thus Gursky and Aleshkov attributed it to Aβ(1-40) monomers and dimers. Our results are consistent with these experimental findings.

Lazo et al. used limited proteolysis with mass spectrometry to identify protease-resistant segments of Aβ(1-40) and Aβ(1-42) [30]. They showed that a ten-residue segment, A21-A30, was protease resistant in both alloforms. Comparing the protease-resistant regions of Aβ(1-40) and Aβ(1-42), they also found that the fragment V36-A42 was protease resistant in Aβ(1-42) only. This result is consistent with previous experimental studies suggesting a β-helix model of Aβ(34-42) fibrils with a turn at G37-G38 stabilized by hydrophobic interactions [31]. This turn structure is in agreement with the solution ^{1}H NMR study of the C-terminal fragment Aβ(34-42) by Weinreb et al., who suggested that this C-terminal hydrophobic cluster nucleates amyloid formation in AD [32]. Our results for monomer conformations are consistent with both these findings because we observe a stable turn structure centered in the region D23-K28 as well as a turn at G37-G38.

Other simulation studies have addressed folding of full-length Aβ. A DMD study by Urbanc et al. using a four-

bead amino acid model with hydrogen bonds and amino acid-specific interactions not only addressed the formation of Aβ(1-40) and Aβ(1-42) oligomers but also studied monomer folding prior to oligomer formation [16]. Results of this study showed that a folded Aβ(1-42) monomer, but not an Aβ(1-40) monomer, possesses a turn at G37-G38 stabilized by a hydrophobic interaction between V36 and V39 [16]. The present study is different from that of Urbanc et al. [16] because the strength of hydrophilic/hydrophobic interactions in our study is smaller, which allows for formation of ordered β-sheet aggregates (Lam et al., unpublished data), and because here we explore temperature dependence and the effects of EI.

An all-atom MD study of helix-to-coil conformational change in Aβ(1-40) monomer was reported by Xu et al., who studied Aβ(1-40) folding in both aqueous and membrane-like environments [33]. In an aqueous solution, Aβ(1-40) trajectories showed an α-helix$\rightarrow$$\beta$-sheet and a β-sheet$\rightarrow$random coil conformational change. In another all-atom MD study of Aβ(1-42) folding in an aqueous solvent at various temperatures and pH conditions, Flöck et al. showed that at least one of the two α-helices is not stable but rather rapidly converts to a random and β-strand-rich conformation [34]. Our results agree qualitatively with the observation in these two studies that Aβ has a propensity to form β-strand-rich conformations in aqueous solution.

Recently, Aβ(1-42) monomer structure was studied by Baumketner et al. using a combination of ion-mobility spectrometry–mass spectrometry and replica exchange MD simulations with implicit water solvent [35]. They showed that Aβ(1-42) did not adopt a unique fold, but rather a mixture of rapidly interconverting conformations that were classified into three distinct families. The secondary structure analysis revealed that these conformations were dominated by loops and turns but that some helical structure formed in the C-terminal hydrophobic tail. Though the method of Baumketner et al. differed significantly from that used here, our results agree reasonably well. We observe not only three families of structures, but many different conformations with similar potential energies at any selected temperature, meaning that more than one folded structure of Aβ(1-42) is possible. These results are consistent with the notion that the Aβ(1-42) monomer possesses little regular order. Baumketner et al. also proposed that the transitory appearance of α-helical structure observed experimentally by Kirkitadze et al. in studies of the assembly of all physiologically-relevant Aβ alloforms known at that time [36], results from association of unstructured monomers into oligomers in such a way that the hydrophobic tails of the peptide become shielded from the solvent. This shielding would create an apolar microenvironment promoting α-helix formation from pre-existing seeds. In agreement with this observation, we also found a small amount of α-helical structure at low temperatures where Aβ(1-42) adopts a collapsed coil structure.

V. CONCLUSIONS

We present structural findings on Aβ(1-42) folding using a DMD approach combined with a four-bead protein model that allows us to explore a wide temperature range and obtain 100 trajectories per temperature. This approach also allows us to vary the EI strength. Our results indicate that in the presence of EI, the β-strand propensity increases, yielding a more compact monomer conformation as quantified by $\bar{R}_g$. We also show the presence of some well-defined structural elements, such as turns centered at G25-S26 and G37-G38. However, the overall folded structure of Aβ(1-42) is not unique. The question of a relative contribution of these two well-structured regions versus the other protein regions to the Aβ(1-42) pathway of oligomer and fibril formation remains to be determined.

[1] J. Hardy and D. J. Selkoe, "The amyloid hypothesis of Alzheimer's disease: Progress and problems on the road to therapeutics." *Science* **297**, 353–356 (2002).

[2] J. Hardy, "Testing times for the "amyloid cascade hypothesis". " *Neurobiol. Aging* **23**, 1073–1074 (2002).

[3] W. L. Klein, W. B. Stine Jr., and D. B. Teplow, "Small assemblies of unmodified amyloid β-protein are the proximate neurotoxin in Alzheimer's disease." *Neurobiol. Aging* **25**, 569-580 (2004).

[4] C. G. Glabe, "Amyloid accumulation and pathogensis of Alzheimer's disease: significance of monomeric, oligomeric and fibrillar Aβ." *Subcell Biochem.* **38**, 167–177 (2005).

[5] D. B. Teplow, A. Lomakin, G. B. Benedek, D. A. Kirschner, and D. M. Walsh, "Effects of β-protein mutations on amyloid fibril nucleation and elongation." in *Alzheimer's Disease: Biology, Diagnosis and Therapeutics*, K. Iqbal, B. Winblad, T. Nishimura, M. Takeda, and H. M. Wisniewski, Editors, John Wiley & Sons Ltd., Chichester, England, 311–319 (1997).

[6] K. N. Dahlgren, A. M. Manelli, W. B. Stine, L. K. Baker, G. A. Krafft, and M. J. LaDu, "Oligomeric and fibrillar species of amyloid-β peptides differentially affect neuronal viability." *J. Biol. Chem.* **277**, 32046–32053 (2002).

[7] D. J. Selkoe, "Alzheimer's disease: Genes, Proteins, and Therapy." *Physiol. Rev.* **81**, 741–766 (2001).

[8] Y. Zhou, C. K. Hall, and M. Karplus, "First-Order Disorder-to-Order Transition in an Isolated Homopolymer Model." *Phys. Rev. Lett.* **77**, 2822–2825 (1996).

[9] Y. Zhou and M. Karplus, "Folding thermodynamics of a three-helix-bundle protein." *Proc. Natl. Acad. Sci. USA* **94**, 14429–14432 (1997).

[10] Y. Zhou, M. Karplus, J. M. Wichert, and C. K. Hall, "Equilibrium thermodynamics of homopolymers and clusters: molecular dynamics and Monte-Carlo simulations of system with square-well interactions." *J. Chem. Phys.* **107**, 10691–10708 (1997).

[11] N. V. Dokholyan, S. V. Buldyrev, H. E. Stanley, and E. I. Shakhnovich, "Discrete molecular dynamics studies of folding of a protein-like model." *Folding and Design* **3**, 577–587 (1998).

[12] Y. Zhou and M. Karplus, "Folding of a Model Three-helix Bundle Protein: A Thermodynamic and Kinetic Analysis." *J. Mol. Biol.* **293**, 917–951 (1999).

[13] N. V. Dokholyan, S. V. Buldyrev, H. E. Stanley, and E. I. Shakhnovich, "Identifying the protein folding nucleus using molecular dynamics." *J. Mol. Biol.* **296**, 1183–1188 (2000).

[14] S. Peng, F. Ding, B. Urbanc, S. V. Buldyrev, L. Cruz, H. E. Stanley, and N. V. Dokholyan, "Discrete molecular dynamics simulations of peptide aggregation." *Phys. Rev. E* **69**, 041908 (2004).

[15] B. Urbanc, L. Cruz, F. Ding, D. Sammond, S. Khare, S. V. Buldyrev, H. E. Stanley, and N. V. Dokholyan, "Molecular Dynamics Simulation of Amyloid-β Dimer Formation." *Biophys. J.* **87**, 2310–2321 (2004).

[16] B. Urbanc, L. Cruz, S. Yun, S. V. Buldyrev, G. Bitan, D. B. Teplow, and H. E. Stanley, "*In silico* study of amyloid β-protein (Aβ) folding and oligomerization." *Proc. Natl. Acad. Sci. USA* **101**, 17345–17350 (2004).

[17] J. M. Borreguero, B. Urbanc, N. Lazo, S. V. Buldyrev, D. B. Teplow, and H. E. Stanley, "Discrete molecular dynamics study of the amyloid β-protein decapeptide Aβ(21-30)." *Proc. Natl. Acad. Sci. USA* **102**, 6015–6020 (2005).

[18] D. C. Rapaport, "*The art of molecular dynamics simulation.*" Cambridge University Press (1997).

[19] A. V. Smith and C. K. Hall, "α-helix formation: discontinuous molecular dynamics on an intermediate-resolution protein model." *Proteins* **44**, 344–360 (2001).

[20] A. V. Smith and C. K. Hall, "Assembly of a Tetrameric α-Helical Bundle: Computer Simulations on an Intermediate-Resolution Protein Model." *Proteins* **44**, 376–391 (2001).

[21] F. Ding, J. M. Borreguero, S. V. Buldyrev, H. E. Stanley, and N. V. Dokholyan, "A Mechanism for the α-helix to β-hairpin transition." *Proteins: Structure, Function, and Genetics* **53**, 220–228 (2003).

[22] J. Kyte and R. F. Doolittle, "A simple method for displaying the hydropathic character of a protein." *J. Mol. Biol.* **157**, 105–132 (1982).

[23] M. Heinig and D. Frishman, "STRIDE: a web server for secondary structure assignment from known atomic coordinates of proteins." *Nucl. Aci. Res.* **32**, W500–W502 (2004).

[24] W. Humphrey, A. Dalke, and K. Schulten, "VMD: visual molecular dynamics." *J. Molec. Graphics* **14**, 33–38 (1996).

[25] Y. Zhang and J. Skolnick, "Scoring Function for Automated Assessment of Protein Structure Template Quality." *Proteins: Structure, Function, and Bioinformatics* **57**, 702–710 (2004).

[26] M. Coles, W. Bicknell, A. A. Watson, D. P. Fairlie and D. J. Craik, "Solution structure of amyloid-β peptide (1–40) in a water-micelle environment. Is the membrane spanning domain where we think it is?" *Biochemistry* **37**, 11064–11077 (1998).

[27] O. Crescenzi, S. Tomaselli, R. Guerrini, S. Salvatori, A. M. D'Ursi, P. A. Temussi, and D. Picone, "Solution structure of the Alzheimer amyloid β-peptide (1–42) in an apolar microenvironment. Similarity with a virus fusion domain." *Eur. J. Biochem.* **269**, 5642–5648 (2002).

[28] S. Zhang, K. Iwata, M. J. Lachenmann, J. W. Peng, S. Li, E. R. Stimson, Y. Lu, A. M. Felix, J. E. Maggio, and J. P. Lee, "The Alzheimer's peptide Aβ adopts a collapsed coil structure in water." *J. Struct. Biol.* **130**, 130–141 (2000).

[29] O. Gursky and S. Aleshkov, "Temperature-dependent β-sheet formation in β-amyloid Aβ_{1-40} peptide in water: uncoupling β-structure folding from aggregation." *Biochim. Biophys. Acta* **1476**, 93–102 (2000).

[30] N. D. Lazo, M. A. Grant, M. C. Condron, A. C. Rigby, and D. B. Teplow, "On nucleation of amyloid β-protein monomer folding." *Prot. Sci.* **14**, 1581-1596 (2005).

[31] N. D. Lazo and D. T. Downing, "Fibril formation by amyloid-β proteins may involve β-helical protofibrils." *J. Pept. Res.* **53** 633–640 (1999).

[32] P. H. Weinreb, J. T. Jarrett, and P. T. Lansbury, Jr., "Peptide models of a hydrophobic cluster at the C-terminus of the β-amyloid protein." *J. Am. Chem. Soc.* **116**, 10835–10836 (1994).

[33] Y. Xu, J. Shen, X. Luo, W. Zhu, K. Chen, J. Ma, and H. Jiang, "Conformational transition of amyloid β-peptide." *Proc. Natl. Acad. Sci. USA* **102**, 5403–5407 (2005).

[34] D. Flöck, S. Colacino, G. Colombo, and A. Di Nola, "Misfolding of the Amyloid β-protein: A Molecular Dynamics Study." *Proteins* **62**, 183–192 (2006).

[35] A. Baumketner, S. L. Bernstein, T. Wyttenbach, G. Bitan, D. B. Teplow, M. T. Bowers, and J.-E. Shea, "Amyloid β-protein monomer structure: a computational and experimental study." *Prot. Sci.*, in press.

[36] M. D. Kirkitadze, M. M. Condron, and D. B. Teplow, "Identification and characterization of key kinetic intermediates in amyloid β-protein fibrillogenesis." *J. Mol. Biol.* **312**, 1103–1119 (2001).